The Pennsylvania State University

The Graduate School

College of Earth and Mineral Sciences

FABRICATION AND CHARACTERIZATION OF BIODEGRADABLE MICROSPHERES FOR APPLICATIONS IN ELECTRICALLY CONDUCTIVE BIOMEDICAL DEVICES

A Thesis in

Materials Science and Engineering

by

Martin Antensteiner

Submitted in Partial Fulfillment
of the Requirements
for the Degree of

Master of Science

December 2015

The thesis of Martin Antensteiner was reviewed and approved* by the following:

Mohammad R. Abidian
Assistant Professor of Bioengineering and Materials Science and Engineering
Thesis Advisor

Carlo G. Pantano
Distinguished Professor of Materials Science and Engineering

Erwin A. Vogler
Professor of Materials Science and Engineering and Bioengineering

Suzanne E. Mohney
Professor of Materials Science and Engineering and Electrical Engineering
Chair, Intercollege Graduate Degree Program in Materials Science and Engineering

*Signatures are on file in the Graduate School

Abstract

A novel method to fabricate uniform, biodegradable microspheres from poly(lactic-*co*-glycolic acid) (PLGA) 85:15 using an electrospraying process is outlined in this thesis. Initial optimization of PLGA solution parameters discovered that 4wt% PLGA in chloroform yielded microstructures with a smooth, spherical morphology. The addition of benzyltriethylammonium chloride (BTEAC, 2% (w/w) PLGA) increased the conductivity of the solution, and reduced the coefficient of variance (CV) for microsphere diameter from >20% to 14%. Furthermore, modifications of applied potential and spinneret-collector separation distances during electrospraying improved the microsphere diameter to 11% CV. The fabrication parameters were finalized by the addition of silicon wafer substrates bearing Ti/Au (10/100nm) dual layer electrodes with 1.5mm diameter working areas. Resulting microspheres had an average diameter of 3.23±0.23µm and showed a 7% CV. This method was then applied to exploratory research in fabricating conductive biomedical devices through the electrochemical polymerization of polypyrrole (PPy) for 1 minute on PLGA microspheres. Electrical Impedance Spectroscopy (EIS) and Cyclic Voltammetry (CVt) was performed using a bare gold reference electrode to characterize the electrical properties. The fabricated conducting polymer-based electrodes showed promising 10% and 23% impedance decreases at 1 kHz and 100 Hz respectively relative to the bare gold reference. The charge storage capacity of these devices was improved over bare gold electrodes by 20%. Based on these observations, the PLGA microsphere fabrication route presented in this thesis shows promise for the development of conductive biomedical devices.

Table of Contents

List of Figures

List of Tables

Acknowledgements

I would like to acknowledge and express my gratitude to my advisor, Dr. Mohammad Reza Abidian, for his tireless dedication to his laboratory family in even the most challenging of times. I would also like to thank my laboratory group members, Milad Khorrami and Fattemeh Fallahianbijan, for their instrumental contributions towards the application of this work. I also am greatly appreciative of the members of the Materials Characterization Laboratory for their insightful conversations, valuable input, and assistance during analysis, specifically Trevor Clark, Julie Anderson, Jeffrey Long, and Amanda Baker. And finally, I would like to thank my family, who has never failed to lift my spirits when the going got tough, so thank you to my little sister Ines, my mother Gabriele, and especially Peter, my father.

Chapter 1 Introduction

The use of biodegradable materials for biomedical applications is a practice that dates back thousands of years to the first uses of natural materials such as collagen to assist in wound closures.[1] In the 1960's, synthetic biocompatible polymers such as polyurethane were explored for biomedical applications, such as heart valves and stents.[2] The steady advancement of these synthetic biopolymers over the past two decades has sparked great interest for applications in the biomedical field, specifically where the polymers were also biodegradable through either hydrolytic processes (e.g. polylactides and polycaprolactone), or through enzyme activity such as with poly(amino acids).[3]

1.1 Overview of Poly(lactic-*co*-glycolic acid)

One of the most widely applicable biodegradable and biocompatible polymers in literature today is poly(lactic-*co*-glycolic acid) or PLGA (Figure 1.1) .[4–6] PLGA is soluble in a wide range of organic solvents, such as chloroform, and is degraded by water through hydrolytic cleavage of ester bonds. It is part of a family of FDA approved linear polymers capable of being synthesized in a wide variety of combinations from constituent acids, with applications such as controlled delivery of pharmaceutical drugs and genetic material including DNA.[7–9] PLGA is mainly identified by monomer ratio (i.e. the PLGA 75:25 copolymer is comprised of 75% lactic acid and 25% glycolic acid monomers).[6] Additionally, PLGA can be identified by stereochemistry (i.e. poly D,L-lactic-*co*-glycolic acid signifies a racemic mixture of D and L enantiomers of the acids). The final properties of PLGA (e.g. mechanical strength, degradation rate, etc.) depend strongly on

the initial molecular weight of the polymer, monomer ratio, stereochemistry, exposure to water, and the temperature at which the polymer is stored.[10,11] Table 1.1 compares several variants of PLGA and shows how selected properties vary based on chemical structure.

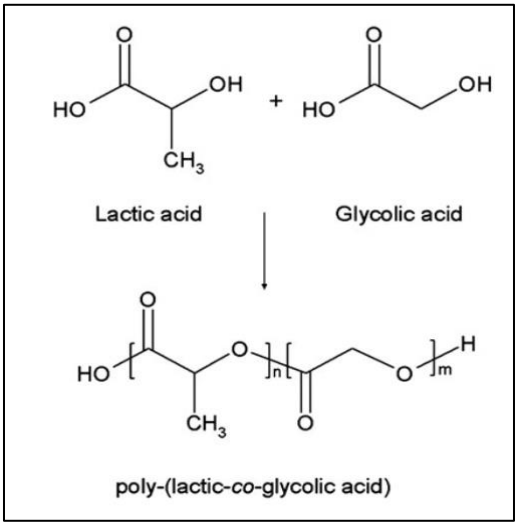

Figure 1.1 Chemical structure of poly(lactic-*co*-glycolic acid) and acid monomers.[6] The subscripts n and m denote monomer ratios, the sum of which is unity.

Table 1.1 Comparison of Selected Biodegradable Polymer Properties[10]

Polymer	Modulus (GPa)	Elongation (%)	Solvent	Cristallinity (%)	Degradation Time (Weeks)
Polyglycolide/ Polyglactine	7.0	15–20	Hexafluoroispropanol	45–55	6–12
Poly(L-lactide)	2.7	-	Benzene, THF, dioxane	37	12–18
Poly(D,L-lactide)	-	3–10	Methanol, DMF	Amorphous	11–15
Poly(D,L-lactide-*co*-glycolide) 85/15	2.0	3–10	Ethyl acetate, chloroform, acetone, THF	Amorphous	5–6
Poly(D,L-lactide-*co*-glycolide) 75/25	2.0	3–10	Ethyl acetate, chloroform, acetone, DMF, THF	Amorphous	4–5
Poly(D,L-lactide-*co*-glycolide) 50/50	2.0	3–10	Ethyl acetate, chloroform, acetone, DMF, THF	Amorphous	1–2
Poly (L-lactide-*co*-glycolide) 10/90	-				

1.2 Conventional Methods for Fabrication of PLGA Microstructures

The encapsulation of bioactive agents such as dexamethasone[12] and bioactive macromolecules such as DNA and RNA[13] is currently one of the most studied applications of PLGA. The wide range of chemical and physical properties available to PLGA allows a substantial degree of flexibility in choosing a fabrication route to create encapsulating microspheres. A few examples of well-known fabrication techniques in literature include emulsions, phase separations, and spray-drying.[14,15] Emulsion methods include single (oil-in-water) and double (water-in-oil-in-water) emulsions, where precise control of the solvents and dispersions is critical to producing uniform microspheres.[16–18] Phase separation (coacervaction) is a more difficult process that requires meticulous control over liquid-liquid interphases and subsequent drying procedures.[19–22] The main advantage here lies in the ability to control size through stirring speed, however, the process is susceptible to agglomerates and uses large quantities of organic solvent. Spray drying is a rapid method involving dispersions or emulsions in a stream of heated air.[23–25] This process excels in simplicity, but also produces a large quantity of agglomerated structures, and suffers from large product loss due to product adhesion to the inner walls of the dryer. The most common drawback for all of the above methods is that produced structures typically have size coefficients of variation (CV) in the range of 10-50%, which is typically too large for reliable performance in biomedical devices.[13]

1.3 Electrospraying as an Alternative Fabrication Method

A fabrication technique that aims to mitigate the disadvantages of conventional methods is known as electrostatic spinning (commonly referred to as electrospinning or

electrospraying)[26]. This technique has seen a significant increase in utilization over the past decade as a simple, cost-effective means of producing continuous nanoscale fibers from polymer solutions.[27] This electrostatic spraying process is based on the uniaxial stretching of a viscoelastic jet of polymer solution or melt.[28,29] A typical laboratory setup for electrospraying is simple, involving only a metallic needle spinneret, a high voltage power supply (typically direct current), and a grounded conductive substrate as a collector (Figure 1.2A). The theory behind the process is more complex however. When an electrical potential (typically 1-30kV) is applied to a polymer solution being pumped through the metallic spinneret, the pendant drop of that solution becomes electrified and is subjected to both electrostatic repulsion from surface charges and coulombic forces from an external electric field generated between the spinneret and grounded collector.[30]

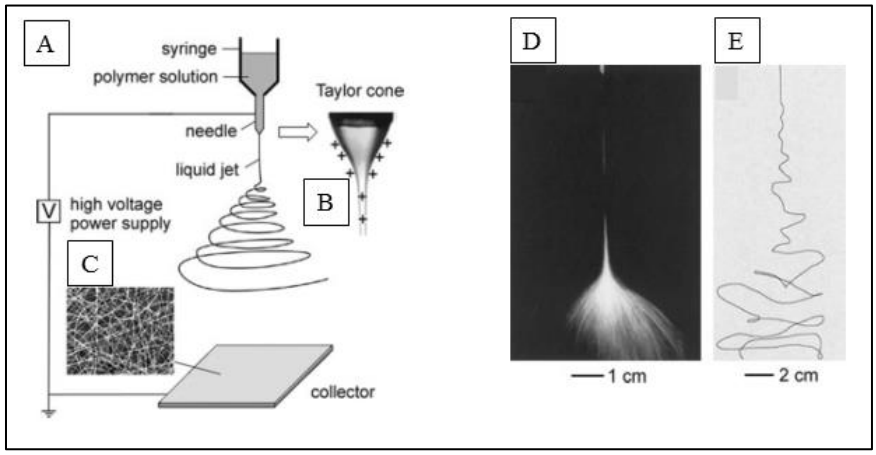

Figure 1.2 A) Schematic of the overall electrospraying process[28], B) Taylor cone formation, and C) the resulting matt of fibers after a typical experiment. D) Image of 1/250 s and E) 18ns timescale photography showing the perceived splitting and actual high frequency whipping behavior of the solution jet.

The surface tension of the viscous polymer solution also influences the process by acting to resist the electrostatic forces applied by the external electric field. Increasing the applied potential to overcome this resistance distorts the pendant solution drop into what

is referred to as the Taylor cone (Figure 1.2B).[31] Further increases in potential will eventually allow the electric field strength to overcome a threshold value of the solution surface tension, resulting in the release of a liquid jet. The jet then undergoes vigorous whipping motions as a result of interactions between the external electric field and surface charges on the jet, which act to decrease the diameter of the ejected fibers as the fiber nears the collector.[32,33] To the naked eye, the ejected fibers give the impression of splitting into many different fibers and forming a wide stream of fibers (Figure 1.2D), but closer inspection with slow-motion photography reveals the whipping phenomenon (Figure 1.2E)[34]. Fibers depositing on the collector typically form a randomly woven matt (Figure 2.1C), as the whipping motion is not conducive to producing aligned fibers. However, the setup and operating conditions of this process can be extensively optimized, granting flexibility in the desired end product such as aligned fibers and intricately woven matts of aligned fibers.[35]

Some common adjustment parameters for the electrospraying process include the applied potential, spinneret-collector separation distance, and solution properties among many others, all of which have been shown to play a role in determining the fabricated morphology of different polymer systems.[27–29] The applied potential directly affects the volume of polymer ejected from the spinneret, as well as the intensity of forces placed on the fiber by the external electric field. The effects of the spinneret-collector separation distance are primarily observed in the final dimensions of the deposited polymers. The greater the distance traveled, the longer the forces applied by the electric field may act on the ejected solution. This is clearly observed during fiber fabrication.[32] Solution properties such as viscosity, surface tension, and solution conductivity are all reported to

affect the morphology of the structures fabricated.[31,35] Agents such as salts are often added to increase the conductivity of the electrosprayed solution and thus increase the forces applied during the spraying process, typically resulting in structures with smaller dimentions[31]. Though fibers are the main microstructures produced from this technique in literature, recent developments have shown the potential for the fabrication of other structures such as microspheres.

1.4 PLGA Microsphere Applications in Electrically Conductive Devices

One potential application of electrospraying is in the fabrication of microelectrode neural probes as demonstrated by Abidian et al[12]. Their work showed the formation of conductive poly(3,4-ethylenedioxythiophene) nanotubes containing PLGA fiber cores created via electrospraying. PLGA performed the dual role of defining the surface area of the subsequent conductive nanotubes while also modifying controlled drug release rates.[12] Nanoscale bioelectronics such as these are in high demand for applications such as neural interfacing[36,37] and bioactuation[38,39], which require small electrode sizes capable of maintaining low impedance characteristics. A persisting challenge for these devices is the electrical impedance, which can become quite large as devices approach the nanoscale. While impedance can be decreased through use of nanofibers with inherently large surface areas, there is potential for further improvement through the use of spherical structures.

The feasibility of creating uniform spherical structures via electrospraying was previously demonstrated with PLGA 50:50.[40] However, those results cannot be directly applied to other PLGA compositions, since as stated above (Section 1.1), the final

morphology depends strongly on solution parameters, including polymer composition[6,27]. Additionally, at the time of this research, no other published literature has tested the electrical impedance and charge storage capacities of conductive electrodes bearing spherical microstructures, which may have significant impacts on the properties of nanoscale bioelectronics.

This thesis describes the optimization of a modified electrospraying process with the ultimate goal of producing well-defined PLGA 85:15 microspheres having diameters approaching the nanometer length scale. The optimized process is then applied to the production of poly(pyrrole) (PPy) electrically conductive electrodes in order to demonstrate the potential of such devices to improve electrical properties for applications in electrically conductive biomedical devices.

Chapter 2 Materials and Methods

2.1 Materials

PLGA (85:15 DLG 7E) with an inherent viscosity of 0.6-0.8 dLg^{-1} was purchased from Evonik Industries (Birmingham, AL). Benzyl-3-triethylammonium chloride (BTEAC) and Pyrrole (molecular weight: 67.09$gmol^{-1}$) were purchased from Sigma-Aldrich. Poly(sodium-p-styrenesulfonate) (PSS, MW 70 kD) was purchased from Acros-Organics. Chloroform ($CHCl_3$) was purchased from SupraSolv Company. N-type silicon wafers coated with TiO_2 were purchased from University Wafer Company. Spinnerets (metal tip, 22 gauge), plastic syringes (3ml), petri dishes (120mm diameter), and plastic microscope slides were purchased from VWR.

2.2 Fabrication of Conductive Substrates

Initial trials used as-purchased plastic microscope slide substrates, which were covered by removable plastic masks. The masks were laser cut (Universal CO_2 Laser Model M360) to the desired "dumbbell" shape as shown below in Section 3.4. The dumbbells were comprised of a square deposition area (0.25cm^2) connect to a larger rectangle (0.25 x 1.0 cm) via a connecting "bridge" (0.1 x 1.0 cm). A one-step sputter coating process (Quorom EMS 150 Sputter Coater) was used to apply a layer of Au (100nm). Later trials used as-purchased N-type semiconductor silicon wafers covered by removable tape masks that were developed for this work. These masks were laser-cut to a different "dumbbell" shape chosen to optimize desired parameters as shown in Section 3.4. The

diameters of the circles were a 1.5mm work area connected to a 5mm circle by a 1.0x10mm "bridge". Masked Si wafers were coated with a dual conductive metal layer comprised of 10nm Ti support layer and 100nm Au to ensure good conductivity and adhesion to the oxide substrate surface (Kurt J. Lesker Lab-18 evaporative coating system). Removal of the plastic slide and removable tape masks respectively completes the substrate fabrication process.

2.3 Fabrication of Electrosprayed Microspheres

The fabrication process for PLGA microspheres was improved in several stages, the methodology of which is presented here in the order utilized. All electrospraying experiments were carried out in a closed Plexiglas box to increase control over the experimental environment.

2.3.1 Initial Fabrication

A homogeneous solution of 3, 4, and 5% (w/w) PLGA was prepared by dissolving 0.473g, 0.617g, and 0.779g of PLGA respectively in 10ml of chloroform at room temperature for 12 hours. The mixture was electrosprayed onto the fabricated plastic substrates described above (Section 2.2) for 25s using an applied field of $100kVm^{-1}$ (10kV applied potential and 10cm spinneret-collector separation distance), a spinneret gauge of 22, and a flow rate of 500µl/hr. Temperature and humidity were controlled at 26°C and 35-37% respectively. The resulting PLGA microspheres were deposited directly onto the $0.25cm^2$ square of the conductive substrate.

2.3.2 Addition of Inert Organic Salt

A homogeneous solution of 3, 4, and 5% (w/w) PLGA and 2% BTEAC (w/w PLGA) was prepared by dissolving aforementioned quantities (Section 2.3.1) of PLGA and 0.0095g, 0.0123g, and 0.0157g BTEAC respectively in 10ml of chloroform at room temperature for 12 hours. The mixture was electrosprayed onto fabricated plastic substrates described above (Section 2.2) for 25s using an applied field of $100kVm^{-1}$ (10kV applied potential and 10cm syringe-substrate separation distance), a spinneret gauge of 22, and a flow rate of 500µl/hr. Temperature and humidity were controlled at 22°C and 30-34% respectively. The resulting BTEAC-loaded PLGA microspheres were deposited directly onto the $0.25cm^2$ square of the conductive substrate.

2.3.3 Optimization of Fabrication Parameters

A homogeneous solution of 4% (w/w) PLGA and 2% BTEAC (w/w PLGA) was prepared by dissolving 0.617g of PLGA and 0.0123g BTEAC in 10ml of chloroform at room temperature for 12 hours. The mixture was electrosprayed onto fabricated plastic substrates described above for 25s. The parameters of field strength ($80kVm^{-1}$, $100kVm^{-1}$, and $133kVm^{-1}$) were tested by varying applied potential and spinneret-substrate separation distance independently. Additionally, an alternative setup to produce $100kVm^{-1}$ was tested (8kV applied potential and 8cm syringe-substrate separation distance). The spinneret gauge was 22, and a flow rate was 500µl/hr. Temperature and humidity were controlled at 25°C and 30-31% respectively. The resulting BTEAC-loaded PLGA microspheres were deposited directly onto the $0.25cm^2$ square of the conductive substrate.

2.3.4 Redesign of Conductive Substrates

The previously used plastic substrates bearing square "dumbbell" electrodes were tested alongside circle "dumbbells" on both plastic and Si wafer substrates. A homogeneous solution of 4% (w/w) PLGA and 2% BTEAC (w/w PLGA) was prepared by dissolving 0.617g of PLGA and 0.0123g BTEAC in 10ml of chloroform at room temperature for 12 hours. The mixture was electrosprayed onto fabricated plastic substrates described above for 25s using an applied field of $100kVm^{-1}$ (8kV applied potential and 8cm syringe-substrate separation distance), a spinneret gauge of 22, and a flow rate of 500µl/hr. Temperature and humidity were controlled at 21°C and 30-31% respectively. The resulting BTEAC-loaded PLGA microspheres deposited directly onto both types of conductive substrate.

2.3.5 Final Optimization of Fabrication Parameters

A homogeneous solution of 4% (w/w) PLGA and 2% BTEAC (w/w PLGA) was prepared by dissolving 0.617g of PLGA and 0.0123g BTEAC in 10ml of chloroform at room temperature for 12 hours. The mixture was electrosprayed onto fabricated plastic substrates described above for 25s using an applied field of $100kVm^{-1}$ (8kV applied potential and 8cm syringe-substrate separation distance), a spinneret gauge of 22, and a flow rate of 500µl/hr. Temperature and humidity were controlled at 22°C and 30-34% respectively. The resulting BTEAC-loaded PLGA microspheres deposited directly onto the 1.5mm circle of the conductive substrate.

2.4. Analysis of Microsphere Morphology

To characterize the size and morphology of the electrosprayed PLGA microspheres, optical bright-field microscopy images were taken at various magnifications (Zeiss Imager Z1, Germany) and analyzed using AxioVision digital processing software. Further analysis was conducted using Field Emission Scanning Electron Microscopy (FESEM) (FEI Helios NanoLab 660 FIB/FESEM). To reduce charging in the FESEM, the samples were briefly sputter coated by gold (Denton Vacuum, LLC) for 40 sec at 40mA.

2.5 Statistical Analysis

Microspheres were analyzed by focusing on a predetermined central area of each optical image and measuring all microspheres within that area. Standard statistical analysis (Origin 8.6 SRO, Northampton, MA) was performed on fabricated PLGA microspheres (n=100-200 microspheres). Outliers were detected and removed by use of a Grubbs Test with a significance of 0.05 (standard two-sided analysis). One-way ANOVA analysis was conducted on Impedance and Cyclic Voltammetry results (OriginPro 2015).

2.6 Conductive Polymer Coating on Fabricated PLGA Microspheres

Exploratory work was completed to test the efficacy of PLGA microspheres as template cores for the fabrication of spherical conductive microstructures from poly(pyrrole) (PPy).

2.6.1 Electrochemical Polymerization of Pyrrole

The electrochemical polymerization of PPy was performed using an Autolab PGSTAT 302N (USA METROHM Company) in galvanostatic mode, with a two-electrode configuration at room temperature. Fabricated PLGA microspheres were coated with a solution of pyrrole (2.0M), which was doped with poly(sodium-p-styrenesulfonate) (PSS) (2.0M) in deionized water using $0.5mAcm^{-2}$ current density for 1 minute. The working electrode was applied to the 5mm circle on the above Si wafer substrates. The counter electrode was connected to a platinum wire in the pyrrole-PSS solution.

2.6.2 Electrochemical Impedance Spectroscopy (EIS)

EIS was used to determine the impedance of PPy-coated and bare gold electrodes. Measurements were done using an Autolab PGSTAT 302N and Nova frequency response analyzer software in potentiostatic mode. A solution of 0.1M phosphate-buffered saline (PBS, pH=7.4) was used as the electrolyte in a three-electrode configuration. The Ag/AgCl reference electrode and PPy-coated microspheres were immersed in the electrolyte along with the counter electrode. An alternating current (AC) sinusoidal signal, with 10mV root-mean-square amplitude, was imposed to measure the impedance magnitude and phase angle over a frequency range of $1\text{-}10^4$ Hz.

2.6.3 Cyclic Voltammetry (CVt)

A staircase CVt was performed using an Autolab PGSTAT 302N with a three-electrode configuration, again using Ag/AgCl as a reference electrode. A scan rate of 30mV s^{-1} was applied, sweeping between -0.8 to 0.4V on the working electrode. The surface area contained inside the CVt curve represents the charge capacity of conducting polymer and was calculated using OriginLab software. In order to calculate the charge storage capacity the third cycle was used since the readings were observed to be consistently stable after the second cycle.

Chapter 3 Results and Discussion

The results of this work are presented in six sections, each showing a progressive step towards optimization of PLGA microsphere fabrication. The first two sections focus on the selection of optimal solution parameters, while the third section deals exclusively with the electric field as controlled by various processing parameters. The fourth section elaborates on substituting the electrode geometry and substrate materials with those that are reported in the literature concerning the intended biomedical device application. The fifth section combines the results of the previous sections to finalize the parameters for the fabrication of PLGA microspheres, with which large quantities of samples are prepared and analyzed. Finally, the sixth section details an exploratory research that combines fabricated microspheres with conductive polypyrrole (PPy) to produce conductive biomedical devices.

3.1 Initial Fabrication of PLGA Microspheres

Studies into various forms of PLGA found that 85:15 lactic/glycolic acids was appropriate for this research due mainly to a high degradation resistance (see Table 1.1). This would allow the fabricated microspheres to withstand subsequent fabrication and characterization steps, which involve exposure to aqueous environments. The processing parameters for initial testing were proposed and are summarized in Table 3.1. The original solvent was dichloromethane, but the high vapor pressure lead to deposition of PLGA precipitate, which often clogged the spinneret. Chloroform was therefore adopted instead. Ambient conditions such as temperature and humidity were difficult to optimize

since the effect on the final product of electrospraying remains uncertain in literature,[27,28,31] however, previous work has found optimum electrospraying conditions between 25-40%. It is difficult to pinpoint why this range is preferable since literature has not formed a consensus, and moreover rarely reports these values. For this thesis, room temperature and ~31% humidity were chosen. The deposition time of 25 seconds consistently yielded samples bearing dense microsphere populations without sphere overlap, and was thus used throughout this research. Unless otherwise stated, each fabrication step was reproduced a minimum of five times, analyzing a minimum of 100 microspheres to calculate statistics.

Table 3.1 Initial Processing Parameters for the Fabrication of PLGA Microspheres

Applied Potential	10kV
Spinneret-Collector Separation Distance	10cm
Deposition Time	25s
Temperature	21 ± 3°C
Humidity	32 ± 2%

Previous work found that a 3-5% PLGA (w/w) concentration range in dichloromethane consistently produced smooth, spherical PLGA microstructures[40], and thus served as a starting point for the work presented in this thesis. It was expected that as solution concentration increased, microsphere diameters would also increase as a result of the amount of polymer deposited per unit time given the same electrospraying conditions.

Figure 3.1 shows representative optical bright-field microscopy images for all three solution concentrations tested in these initial trials. At first glance, fabricated microspheres appeared uniform at all concentrations; however, statistics showed that the average diameters of the microspheres were far from uniform with coefficients of variance (CV) exceeding 20% in all solutions (Table 3.2). Interestingly, there was no distinguishable difference in microsphere diameter between 3, 4, and 5wt% PLGA, in contrast to what was predicted previously[40].

These results indicated that the chosen solution range consistently produced spherical microstructures; however, the observed variance of microsphere diameters at all solution concentrations prompted additional solution modification through the addition of an inert stand-in for the pharmaceutical agents typically carried by PLGA in literature. This addition would increase solution conductivity, theoretically decreasing the microsphere size[32]. The next phase of development therefore concentrated on the addition of such a compound.

Table 3.2 Comparison of Fabricated PLGA Microsphere Diameters

PLGA Concentration	Microsphere Diameter	Coefficient of Variance
3wt%	5.82±1.63μm	28%
4wt%	5.93±1.41μm	23%
5wt%	4.61±1.95μm	43%

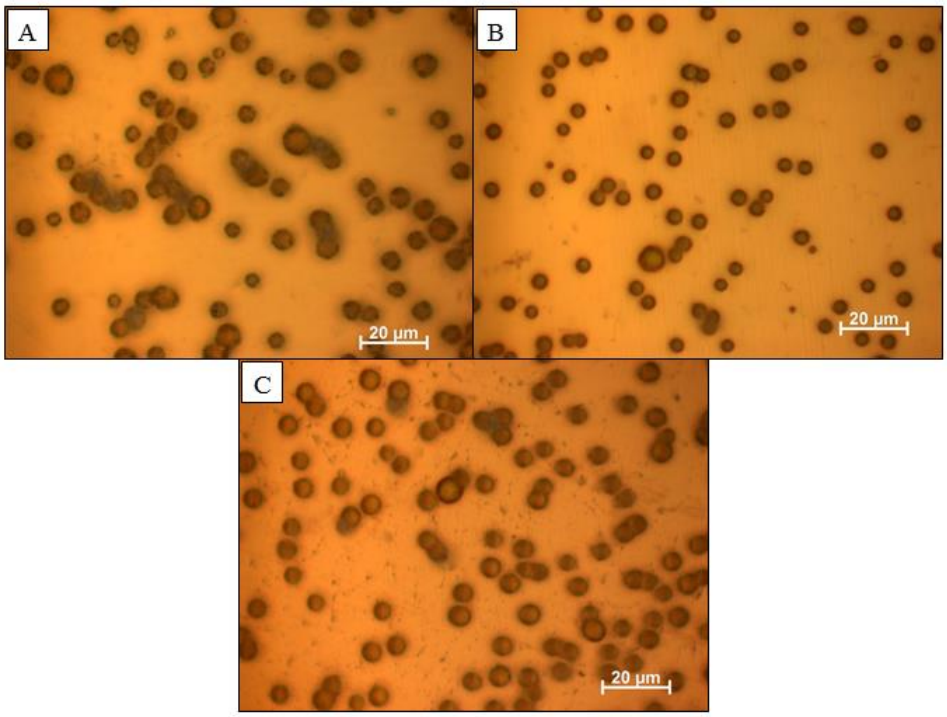

Figure 3.1 Optical bright field images of PLGA microspheres electrosprayed from solutions of A) 3wt%, B) 4wt%, and C) 5wt% PLGA concentrations in chloroform. Microstructures appear consistently spherical in these images; however, low uniformity was evidenced by statistical analysis, prompting further optimization.

3.2 Addition of Inert Organic Salt

The compound chosen for this fabrication route was the inert organic salt benzyl-3-triethylammonium chloride (BTEAC). Based on previous literature[40], a concentration of 2% BTEAC (w/w PLGA) was added to the above solutions (Section 3.1). Figure 3.2 shows the optical images comparing microspheres resulting from the three solutions. The addition of BTEAC was observed to decrease the diameters of the resulting microspheres, and also had an intriguing impact on resulting morphology.

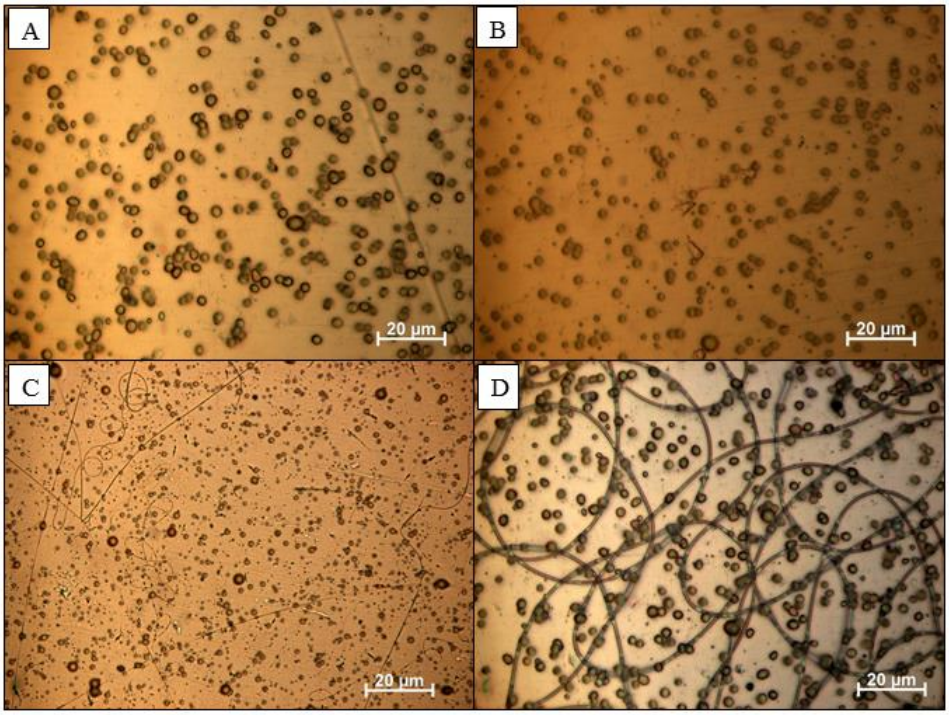

Figure 3.2 Optical bright field images of PLGA microspheres electrosprayed from solutions of A) 3wt%, B) 4wt%, and C) 5wt% PLGA concentration in chloroform with 2% BTEAC (w/w PLGA). Samples from 5wt% and D) 3wt% solutions often showed morphologies such as fibers, while 4wt% rarely contained such structures.

The results of the 3wt% solution (Figure 3.2A) were initially promising based on the statistical analysis of the microsphere diameters (Table 3.3), which indicated a 12% CV. However, it was difficult to reproduce these results in subsequent experiments. Large fibers were frequently found among the microspheres as shown in Figure 3.2D.

Table 3.3 Comparison of Fabricated PLGA/BTEAC Microsphere Diameters

PLGA Concentration	Microsphere Diameter	Coefficient of Variance
3wt%	2.91±0.35µm	12%
4wt%	2.82±0.41µm	15%
5wt%	-	-

Figure 3.2B shows the results from the 4wt% PLGA solution, which appeared uniform and essentially free of fibers. Statistics reveal a much narrower diameter distribution than previously obtained for 4wt% PLGA (Section 3.1). The samples prepared from 5wt% PLGA were far less promising owing to the persistent presence of fibers. As a result, no statistical data was taken, and this solution was deemed unsuitable for further optimization. Overall, the addition of salt proved feasible for CV reduction, but also increased the presence of fiber structures in 3 and 5 wt% PLGA solutions. Further optimization was therefore limited to 4wt% PLGA and shifted focused to process parameters.

3.3 Optimization of Fabrication Parameters

As determined in the previous experiments, the solution parameters for 4wt% PLGA with 2% BTEAC (w/w PLGA) in chloroform were effective for producing microspheres, but further adjustments to processing parameters were needed to narrow the diameter distributions. Solution flow rate and the spinneret gauges are often stated to influence final polymer morphology[28], but were not found to have a consistent impact the results of this research. Thus, a 500µl/hr flow rate and spinneret gauge of 22 was chosen based on previous research and are held constant for the work presented in this thesis.

The most influential parameter of the electrospraying process perhaps is the electric field strength when generated between the spinneret and the grounded collector. As mentioned above (Section 1.3), the electric field can be affected by alterations in the applied potential and the spinneret-collector separation distance. In this section, the effects of varying these parameters were analyzed using 4wt% PLGA with 2% BTEAC

(w/w PLGA) solution. Figure 3.3 shows the effect of both a lower (80kVm^{-1}) and higher (133kVm^{-1}) field strength than used in the previous sections (100kVm^{-1}). Here, the density of deposited microspheres appears to increase with electric field strength. At a low field strength (Figure 3.3A), the diameter of the microspheres was 2.89±0.33µm, approximately the same size as in previous trials (Section 3.2). The use of a higher field strength (Figure 3.3B) had no significant ($p>>0.05$) impact on microsphere diameter (2.90±0.38µm).

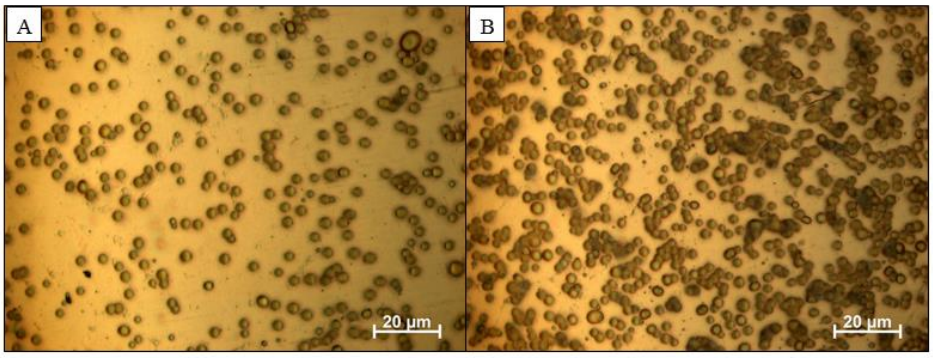

Figure 3.3 Optical bright field images of PLGA microspheres electrosprayed from 4wt% PLGA with 2% BTEAC (w/w PLGA) solutions. The strength of the electric field was varied between A) 80kVm^{-1} and B) 133kVm^{-1}. Microsphere density was observed to increase with the applied field strength, though microsphere diameter was not impacted.

Though uniform microspheres were produced (~13% CV), it was difficult to prevent the simultaneous formation of other microstructures. Lower field strengths imparted lower forces on the PLGA solution, often resulting in large drops of solvent interspersed with microspheres as seen in Figure 3.4A. Conversely, higher electric field strength resulted in frequent fiber formation as shown in Figure 3.4B. Such features were notably less frequent at the previously tested electric field strength of 100kVm^{-1}, leading to the hypothesis that the electric field may not be consistent between the substrate and spinneret. Therefore, the spinneret-collector separation distance was decreased to 8cm,

requiring a reduction of applied potential to 8kV to maintain a 100kVm^{-1} applied field. The shorter distance was predicted to mitigate possible interference of the electric field or interactions occurring between sprayed droplets that may have been responsible for the other microstructures observed earlier. Figure 3.5 shows the results of this adjustment.

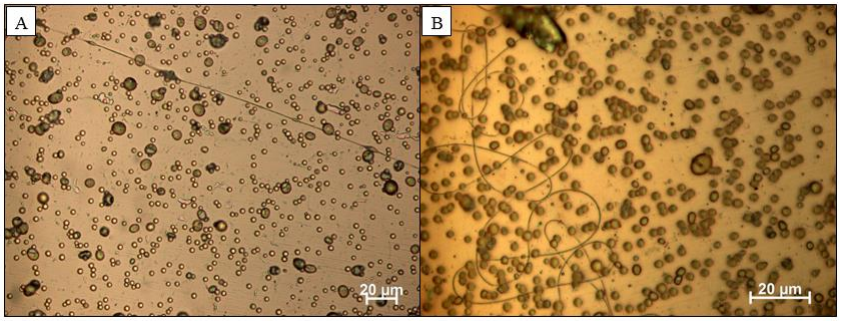

Figure 3.4 Optical bright field images of PLGA microspheres electrosprayed from 4wt% PLGA and 2% BTEAC (w/w PLGA) solutions. The strength of the electric field was varied between A) 80kVm^{-1}, which is susceptible to large droplet formation and B) 133kVm^{-1}, which produced fibers on a consistent basis.

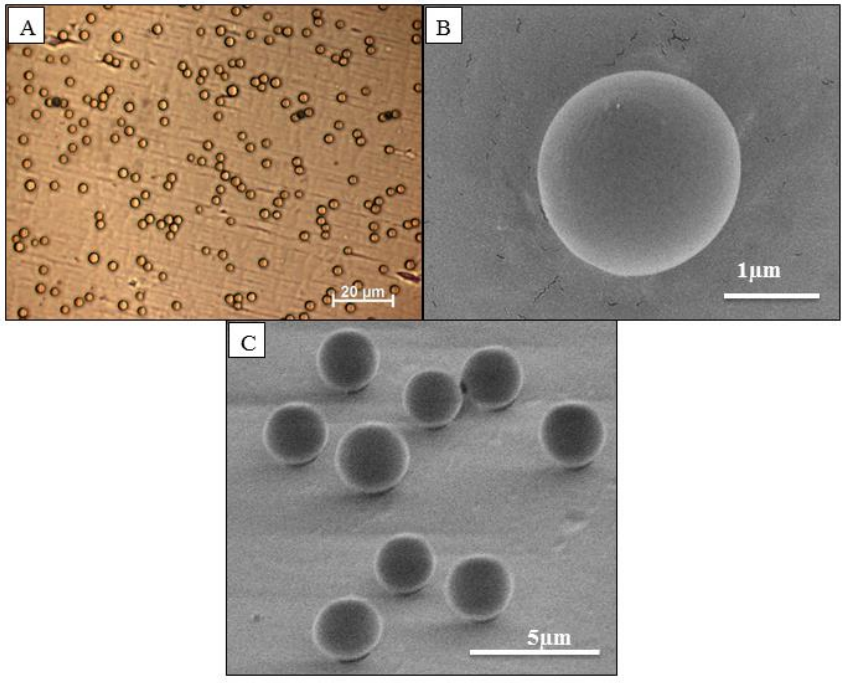

Figure 3.5 A) Optical and B,C) FESEM images of PLGA microspheres electrosprayed from 4wt% PLGA and 2% BTEAC (w/w PLGA) solutions at 100kVm^{-1} electric field strength (8kV applied potential, 8cm spinneret-collector separation distance). Microspheres appear smooth and uniform in the optical images; an observation confirmed by FESEM images.

As shown in Figure 3.5A, the structures produced from the 100kVm^{-1} applied electric field and shorter spinneret to substrate separation distance lack the fibers or droplets observed previously. Statistical analysis shows that these microspheres had diameters of 3.55±0.4μm and 11% CV. Additional imaging with Field-Emission Scanning Electron Microscopy (FESEM) confirms a smooth, spherical geometry for the deposited microspheres. These results appear to support the previously stated hypothesis of electric field inconsistency. The next step in development was to mass produce these microspheres for applications in biomedical devices. However, the electrode substrates used thus far were simple plastic coverslips with a large square area of sputtered gold, and are generally unsuitable for bioelectronics applications, as explained in the next section.

3.4 Redesign of Conductive Substrates

For the intended application of these PLGA microspheres in bioelectronics, smaller electrode sizes are favored as they minimize undesired biological responses such as fibrous encapsulation and inflammatory responses. Since the work described here is intended to be applied to such electrodes, decreasing the electrode size was considered prudent. Figure 3.6 shows the alteration from a square area of interest (Figure 3.6A) to a smaller circular one (Figure 3.6B).

Figure 3.7 shows the results of employing the solution and processing parameters from the previous sections on the smaller electrodes. While the morphology and diameter of the microspheres appeared uniform, the density of these deposited structures varied greatly from the edge of the gold electrode to the center. Further, the shape of the

deposition area did not follow any distinguishable pattern (Figure 3.7A,B) and changed on a per sample basis. Figure 3.6B also shows this phenomenon through the irregular pattern on the electrode area of interest (red circle).

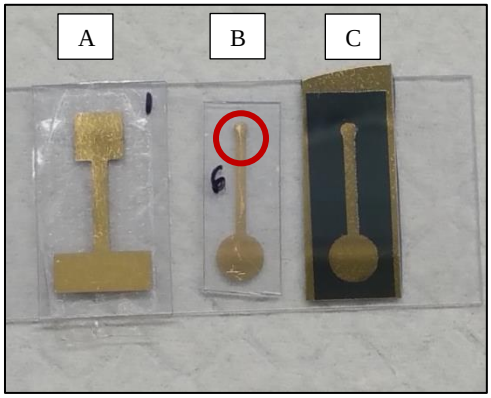

Figure 3.6 Image showing the progression of electrode substrates from the A) initial square shape to B) the final circular configuration. The red circle highlights the irregular deposition of PLGA microspheres on the electrode (light cream color). C) The final electrode shape on Si wafer substrates.

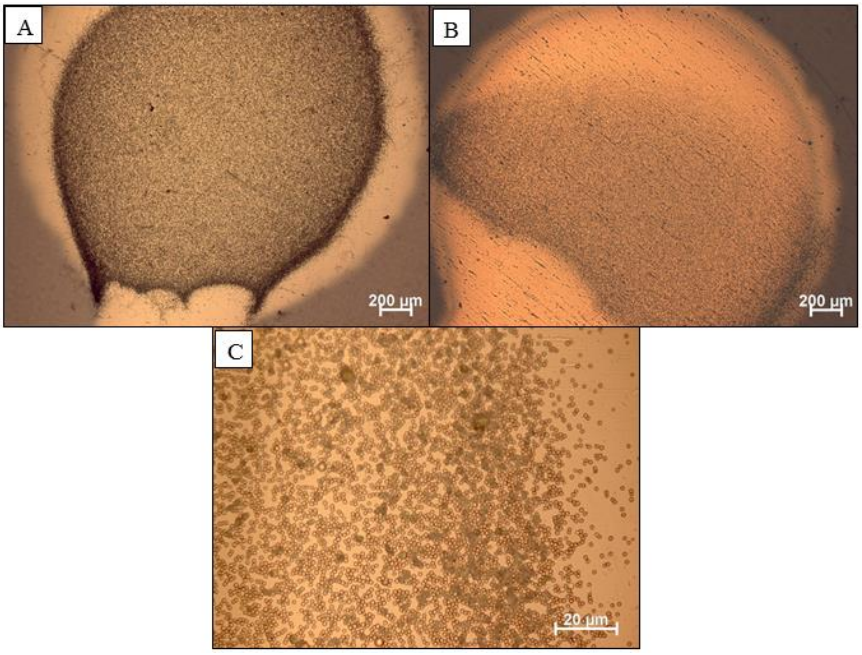

Figure 3.7 Optical bright field images of PLGA microsphere deposition patterns on plastic substrates bearing circular electrodes. A) and B) show the irregularity of the deposition area while C) shows higher magnification of the density distribution from the outer edge of the deposition area to the center. Electric field edge effects may be the cause of the unpredictable pattern and high density of microspheres at the edge of the gold electrode.

This lack of control and severity of microsphere density changes near the electrode edge may be attributed in part to electric field edge effects. Since the plastic substrate is insulating, the electric field is generated only in the area designated by the gold electrode shape, increasing the complexity of the process. Similar effects were previously observed for the large square electrodes, though this phenomenon had little impact on PLGA deposition patterns on the relatively large electrodes. It was hypothesized that switching to a semiconductor substrate may mitigate this problem. Silicon semiconductor substrates are ideal substitutes for the plastic substrates on account of their wide applicability in the electronics industry and literature[36]. A sample of this new substrate is shown in Figure 3.6C. Switching to silicon, however, introduced new challenges. Gold is notoriously poor at wetting the surface of silicon wafers, thus requiring an additional layer of titanium to ensure proper adhesion. Instead of traditional sputter coating, an evaporative sputtering technique was adopted. The plastic masks used previously were ill-suited for such a process and thus necessitated a new fabrication route for masks as is described in Section 2.2.

Figure 3.8 shows the results of combining the solution and process parameters developed in previous sections with the new substrate shape and material. While the adhesive masks were not ideal and yielded rough edges on the electrodes, deposited microspheres did not have preference for either the gold electrode or the silicone substrate. This result supports the earlier hypothesis of electric field edge effects disrupting uniform deposition on plastic substrates. Moreover, the uniformity of the microsphere sizes was maintained, and other morphologies such as fibers were almost

completely excluded. Based on these results, the fabrication route for PLGA microspheres could be applied to mass produce samples for subsequent application.

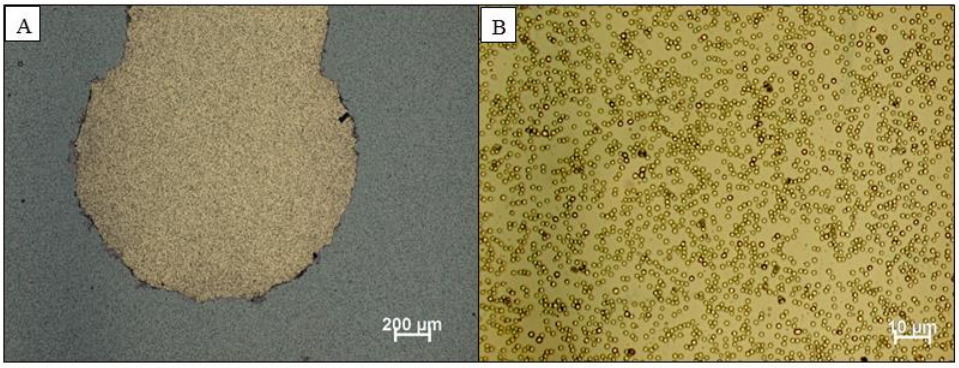

Figure 3.8 Optical bright field microscopy images of PLGA microsphere distributions on silicon wafer substrates at A) 5X and B) 50X. Though the electrode edges were rough in appearance, microsphere deposition was not affected and had no distinguishable preference for either gold or silicon surfaces.

3.5 Final Optimization of PLGA Microsphere Fabrication Parameters

This section summarizes large scale production of PLGA 85:15 microspheres with encapsulated 2% BTEAC (w/w PLGA) as a stand-in for anti-tumor or anti-inflammatory agents. The processing and solution parameters refined in the previous four sections are summarized in Table 3.4.

After coating over 50 samples, statistical data was collected from ten samples chosen at random from the population. The central points of those images were magnified six times, leaving generally 15-25 microspheres within those boundaries for a total of 200, all of which were counted and measured according to Section 2.5. Figure 3.9 shows optical and FESEM images typical of the samples produced. The deposited structures appear as smooth spheres with even density distributions across the electrode surface.

Table 3.4 Final Parameters for the Electrospraying of PLGA Microspheres

Polymer	PLGA 85:15
Solvent	Chloroform
Conductivity Modifier	BTEAC Organic Salt
Solution Concentration	4wt% PLGA/2wt%BTEAC
Applied Potential	8kV
Spinneret-Substrate Separation Distance	8cm
Electric Field Strength	100kV/m
Flow Rate	500µl/hr
Deposition Time	25s
Ambient Temperature	22°C
Ambient Humidity	32%
Spinneret Gauge	22

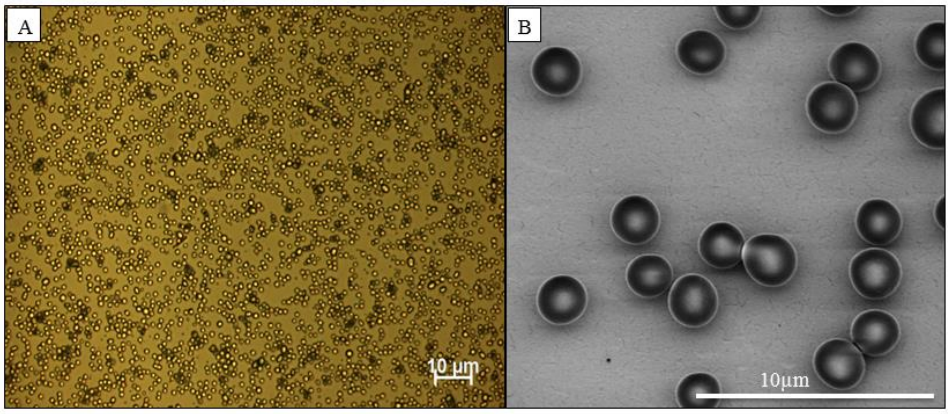

Figure 3.9 Representative A) optical and B) FESEM images of the PLGA microspheres fabricated by the optimized electrospraying process.

Figure 3.10 gives a histogram showing the diameter distribution of these microspheres. The average microsphere diameter was 3.23±0.23µm, with a 7% CV. This is the lowest diameter variance achieved by this work and can be considered a substantial

improvement from the initial experiments. The process can now be applied to bioelectrical device fabrication, a brief example of which is given in the next section.

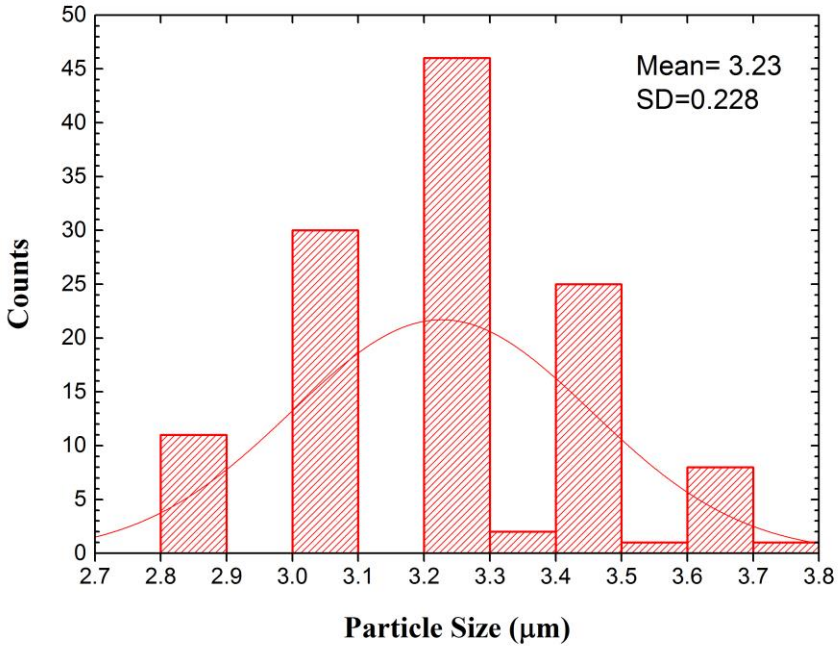

Figure 3.10 Histogram showing the distribution of PLGA microsphere sizes produced during the mass production step of this work. The average microspheres diameter was 3.23±0.23μm, with a 7% CV.

3.6 Conductive Polymer Coating on Fabricated PLGA Microspheres

The results from the previous sections showed that PLGA can be readily processed into spherical microstructures. Additionally, it was previously shown that PLGA 85:15 is stable during electrochemical polymerization and can be removed via dissolution in chloroform, leaving surrounding structures intact, thus making it desirable for applications with conducting polymer structures[12,41] A preliminary experiment combining the fabricated microspheres from Section 3.6 is detailed here.

The Electrodes bearing electrosprayed PLGA microspheres were placed in a solution of the conductive monomer pyrrole and dopant ionic salt poly(sodium-p-styrenesulfonate) (PSS) in deionized (DI) water. Electrochemical polymerization was carried out according to the procedure given in Section 2.6.1. Figure 3.11 shows FESEM images of a 1 min coating of PPy. Optical images were not obtained, since polymerized polypyrrole (PPy) does not transmit or reflect enough light for practical observations.

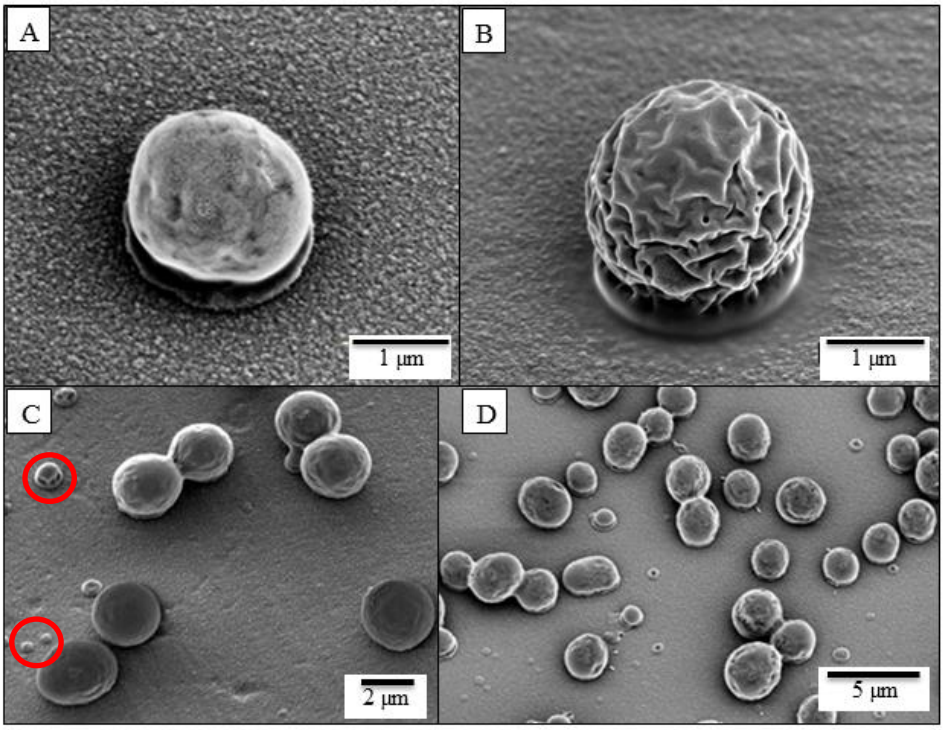

Figure 3.11 FESEM images of A, B) individual and C, D) multiple PLGA microspheres partially encapsulated by conductive PPy. Defects on the surface of the microspheres were plausibly due to electron beam damage. The red circles in C) highlight instances where PPy coating encapsulates smaller structures, indicating complete encapsulation of all microspheres is plausible given longer polymerization times.

The rougher surface surrounding the microspheres seen in Figure 3.11 is indicative of a PPy film since FESEM images without any PPy coating (Figure 3.9B) show the characteristic grain structure of gold around the microspheres. The coating

process initiated from the gold substrate and surrounded the bottom of the PLGA microspheres first, likely a result of the electrochemical polymerization process itself, which occurs at the interface of a conductive substrate and the monomer solution.[42] Since the PLGA microspheres are insulating in nature, PPy tends to deposit first around the bottoms of these microspheres. The precise polymerization mechanism is still debated in literature.[42,43] It is predicted that given longer polymerization times, the coating will continue to encapsulate the microspheres until they are completely covered, as is evidenced by some of the smaller structures in Figure 3.11C (red circles).

The electrical performance of these conductive microstructures was measured in the form of Electrical Impedance Spectroscopy (EIS) and Cyclic Voltammetry (CVt). These characterization techniques are widely accepted in literature and are described in full detail elsewhere[44–46], therefore, only a basic summary of each technique is provided.

Resistance is a measure of a circuit component's ability to resist the flow of electrical current, and is restricted to circuits that follow Ohm's Law $\left(R = \frac{E}{I}\right)$ where resistance (***R***) (ohms) is defined as the ratio of potential (***E***) (volts) to current (***I***) (amperes). More complex circuits and situations involving alternating currents (AC), such as those detailed in this thesis, require a more general resistance parameter called impedance. EIS measures the impedance of a circuit by applying a range of small AC potentials to a circuit and calculating the resulting impedance (***Z***) (ohms) based on Equation 3.1,

Equation 3.1
$$Z = \frac{E_t}{I_t} = \frac{E_0 \sin(\omega t)}{I_0 \sin(\omega t + \varphi)} = Z_0 \frac{\sin(\omega t)}{\sin(\omega t + \varphi)}$$

where (***E***) and (***I***) are as defined above, (***ω***) is the radial frequency in hertz, (***t***) is time, and (***φ***) is the phase shift between applied and measured signals at time ***t***. Subscripts indicate applied ($_0$) and measured signals at time ***t*** ($_t$). Data is typically presented as a log-log plot of impedance vs. AC frequency.

CVt applies a cyclic potential to a system that sweeps first towards a negative and subsequently back towards a positive potential value. The current resulting from the applied potential is then measured and analyzed. In a typical experiment, the negative potential increases the measured current until reduction within in the system occurs. As the potential sweeps towards positive values, a second peak appears when a part of the system oxidizes. The frequency and potential range at which peaks occur depend on the system being analyzed. A full sweep encloses a derived surface area, which in this thesis is used to calculate the charge storage capacity of the system as shown below.

Figure 3.12 shows the results of both types of analysis on a bare reference electrode, and one bearing PLGA microspheres coated with PPy for 1 minute. For each type of analysis, five samples were compared and averaged.

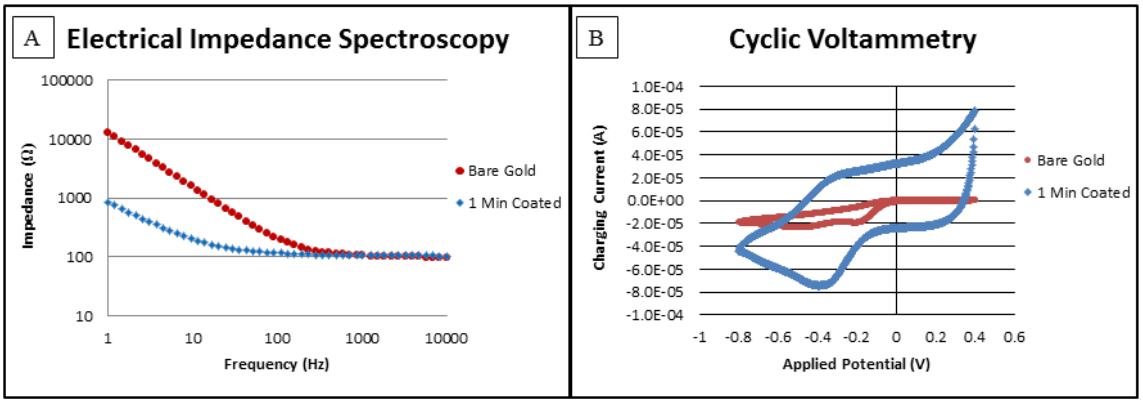

Figure 3.12 A) EIS spectroscopy and B) CVt comparing bare gold reference samples and electrodes bearing PLGA microspheres coated for 1 min with PPy.

The EIS data (Figure 3.12A) shows a large decrease in impedance when compared to bare gold at the low end of the frequency spectrum. For relevant bioelectronics applications, it is common practice to examine impedance at specific frequencies relevant to the intended application[37]. For this work, the impedance at 110Hz and 1kHz were compared between the fabricated sample and the gold reference. At 110 Hz, the fabricated sample impedance significantly ($p<0.05$) decreased from 165±14Ω to 127±10Ω, an improvement of 23%. At 1kHz, the fabricated sample also showed a significant ($p<0.05$) decrease of 10% in impedance from 100±10Ω to 90±10Ω. These results show potential for continued improvement of impedance properties given longer electrochemical polymerization durations.

CVt data shows improvement in terms of charge-storage capacities over the bare gold substrates (Figure 3.12B). CVt was measured in order to determine the absolute charge storage capacity of the fabricated devices, which is directly related to the surface area contained within the CVt plot as shown in Equation 3.2.

Equation 3.2

$$\boldsymbol{Q = \frac{S}{r * A}}$$

In the above equation, (***Q***) is the charge-storage capacity (C/cm^2), (***S***) is the derived surface area of the CVt plot (See Section 2.6.2), (***r***) is the scanning rate (V/s), and (***A***) is the absolute surface area of the electrode (cm^2). As seen in the figure above, the coated electrode had a dramatically larger area (***S***) than the bare gold. Calculations show a significant ($p<0.05$) improvement in charge storage capacity from 1.89± $0.33mC/cm^2$ to $2.31±0.55mC/cm^2$. This result holds promise that long durations of coating with PPy can further improve the storage capacity.

Chapter 4 Conclusions and Future Work

This work discloses the development of a novel fabrication route to produce uniform PLGA 85:15 microspheres on the surface of effective electrodes for potential applications in electrically conductive bioelectronics devices. Previous works by other groups provided inspiration for the initial fabrication of well-defined structures ranging from nanofibers to microspheres, but no previous work incorporated PLGA 85:15, a polymer with higher resistance to hydrolysis. Further, PLGA microspheres had yet to be combined with conductive polymers for bioelectronics applications.

Initial fabrication steps taken from the literature did not produce monodisperse microspheres (CV>20%), and occasionally produced a variety of other structures including fibers and large solvent drops. The addition of an organic salt, BTEAC improved the CV to ~14% in diameter for 4wt% PLGA solutions containing 2% BTEAC (w/w PLGA). Modification of the applied electric field strength above and below $100 kVm^{-1}$ did not reliably improve fabricated microsphere uniformity. However, decreasing the applied potential to 8kV and the spinneret-substrate separation distance to 8cm decreased CV to 11%. The replacement of plastic substrates and larger square electrodes with silicon wafer substrates bearing small circular electrodes yielded further improvement of the microsphere sizes and uniformity. Mass production using the settings determined from all previous steps resulted in uniform microspheres with diameters in the range of 3.23±0.23µm (CV=7%).

The potential application for bioelectronics devices was demonstrated through exploratory research where PLGA microspheres were coated with a layer of electrochemically polymerized conducting PPy for one minute. The electrical properties of impedance and charge-storage capacity were tested using EIS and CVt analysis. Impedance testing showed statistically significant ($p<0.05$) decreases at 110Hz and 1kHz frequencies (23% and 10% decrease respectively) when compared to bare gold references. CVt analysis also showed statistically significant ($p<0.05$) improvements in charge storage capacity nearing 20% over bare gold electrodes, a promising value considering the small amount of PPy deposited.

Additional work may be useful to further refine the fabrication process and broaden the applicability of this technology. The substitution of BTEAC for more biologically-relevant agents such as anti-tumor or anti-inflammatory pharmaceuticals may allow the PLGA microspheres produced by this method to address a wide range of medical conditions. Continuation of the PPy coating as a function of deposition time will likely find further improvement of the impedance and charge-storage capacities of the overall electrode. Further, nearly complete coating of the PLGA microspheres with PPy followed by subsequent removal of PLGA may yield optimum electrical properties due to the additional surface area inside the now hollow microstructures. While microstructures prove effective, the development of controllable structures at the nanoscale is highly desirable and remains a challenge. Future work with this process may lead to the development of PLGA nanospheres as templates for nanostructured bioelectronics.

References

1. Nair, L. S. & Laurencin, C. T. Biodegradable polymers as biomaterials. *Prog. Polym. Sci.* **32,** 762–798 (2007).

2. Ratner, B. D., Hoffman, A. S., Shoen, F. J. & Lemons, J. E. *Biomaterials Science.* (Elsevier, 2013). doi:10.1016/B978-0-08-087780-8.00154-6

3. Tian, H., Tang, Z., Zhuang, X., Chen, X. & Jing, X. Biodegradable synthetic polymers: Preparation, functionalization and biomedical application. *Prog. Polym. Sci.* **37,** 237–280 (2012).

4. Hirenkumar, M. K. & Siegel, S. J. Poly Lactic-co-Glycolic Acid (PLGA) as Biodegradable Controlled Drug Delivery Carrier. *Polymers (Basel).* **3,** 1377–1397 (2011).

5. Wu, X. S. Synthesis, Chraracterization, Biodegradation and Drug Delivery Application of Biodegradable Lactic/ Glycolic Acid Polymers : Part III . Drug Delivery Application. *Artif. Cells, Blood Substitutes Biotechnol.* **32,** 575–591 (2004).

6. Gentile, P., Chiono, V., Carmagnola, I. & Hatton, P. V. An overview of poly(lactic-co-glycolic) acid (PLGA)-based biomaterials for bone tissue engineering. *Int. J. Mol. Sci.* **15,** 3640–59 (2014).

7. Mogi, T., Ohtake, N., Yoshida, M. & Chimura, R. Sustained release of 17b-estradiol from poly (lactide-co-glycolide) microspheres in vitro and in vivo. **17,** 153 – 165 (2000).

8. Soppimath, K. S., Aminabhavi, T. M., Kulkarni, a R. & Rudzinski, W. E. Biodegradable polymeric nanoparticles as drug delivery devices. *J. Control. Release* **70,** 1–20 (2001).

9. Hans, M. . & Lowman, A. . Biodegradable nanoparticles for drug delivery and targeting. *Curr. Opin. Solid State Mater. Sci.* **6,** 319–327 (2002).

10. Houchin, M. L. & Topp, E. M. Physical properties of PLGA films during polymer degradation. *J. Appl. Polym. Sci.* **114,** 2848–2854 (2009).

11. Anderson, J. M. & Shive, M. S. Biodegradation and biocompatibility of PLA and PLGA microspheres. *Adv. Drug Deliv. Rev.* **64,** 72–82 (2012).

12. Abidian, M. R., Kim, D. H. & Martin, D. C. Conducting-polymer nanotubes for controlled drug release. *Adv. Mater.* **18,** 405–409 (2006).

13. Jain, R. A. The manufacturing techniques of various drug loaded biodegradable poly(lactide-co-glycolide) (PLGA) devices. *Biomaterials* **21,** 2475–2490 (2000).

14. Astete, C. E. & Sabliov, C. M. Synthesis and characterization of PLGA nanoparticles. *J Biomater Sci Polym Ed* **17,** 247–289 (2006).

15. Mundargi, R. C., Babu, V. R., Rangaswamy, V., Patel, P. & Aminabhavi, T. M. Nano/micro technologies for delivering macromolecular therapeutics using poly(d,l-lactide-co-glycolide) and its derivatives. *J. Control. Release* **125,** 193–209 (2008).

16. Dunne, M., Corrigan, O. I. & Ramtoola, Z. Influence of particle size and dissolution conditions on the degradation properties of polylactide-co-glycolide particles. *Biomaterials* **21,** 1659–1668 (2000).

17. Zhang, Y., Chan, H. F. & Leong, K. W. Advanced materials and processing for drug delivery: The past and the future. *Adv. Drug Deliv. Rev.* **65,** 104–120 (2013).

18. Spenlehauer, G., Vert, M., Benoit, J. P. & Boddaert, A. In vitro and In vivo degradation of poly(D,L lactide/glycolide) type microspheres made by solvent evaporation method. *Biomaterials* **10,** 557–563 (1989).

19. Lee, T. H., Wang, J. & Wang, C. H. Double-walled microspheres for the sustained release of a highly water soluble drug: Characterization and irradiation studies. *J. Control. Release* **83,** 437–452 (2002).

20. Pekarek, K. J., Jacob, J. S. & Mathiowitz, E. Double-walled polymer microspheres for controlled drug release. *Nature* **367,** 258–60 (1994).

21. Thomasin, C., Nam-Trân, H., Merkle, H. P. & Gander, B. Drug microencapsulation by PLA/PLGA coacervation in the light of thermodynamics. 1. Overview and theoretical considerations. *J. Pharm. Sci.* **87,** 259–268 (1998).

22. Thomasin, C., Merkle, H. P. & Gander, B. Drug Microencapsulation by PLA / PLGA Coacervation in the Light of Thermodynamics . 2 . Parameters Determining Microsphere Formation. *J. Pharm. Sci.* **87,** 269–275 (1998).

23. Ermis, D. Ë. & Yuksel, A. Perparation of spray-dried microspheres of indomethacin and examination of effects of coating on dissolution rates. *J. Microencapsulations* **16,** (1999).

24. Berkland, C., King, M., Cox, A., Kim, K. & Pack, D. W. Precise control of PLG microsphere size provides enhanced control of drug release rate. *J. Control. Release* **82,** 137–147 (2002).

25. Mu, L. & Feng, S. S. Fabrication, characterization and in vitro release of paclitaxel (Taxol) loaded poly (lactic-co-glycolic acid) microspheres prepared by spray drying technique with lipid/cholesterol emulsifiers. *J. Control. Release* **76,** 239–254 (2001).

26. Huang, Z. M., Zhang, Y. Z., Kotaki, M. & Ramakrishna, S. A review on polymer nanofibers by electrospinning and their applications in nanocomposites. *Compos. Sci. Technol.* **63,** 2223–2253 (2003).

27. Greiner, A. & Wendorff, J. H. Electrospinning: A fascinating method for the preparation of ultrathin fibers. *Angew. Chemie - Int. Ed.* **46,** 5670–5703 (2007).

28. Li, D. & Xia, Y. Electrospinning of nanofibers: Reinventing the wheel? *Adv. Mater.* **16,** 1151–1170 (2004).

29. Pham, Q. P., Sharma, U. & Mikos, A. G. Electrospinning of polymeric nanofibers for tissue engineering applications: a review. *Tissue Eng.* **12,** 1197–211 (2006).

30. Reneker, D. H. & Chun, I. Nanometre diameter fibres of polymer, produced by electrospinning. *Nanotechnology* **7,** 216–223 (1999).

31. Bhardwaj, N. & Kundu, S. C. Electrospinning: A fascinating fiber fabrication technique. *Biotechnol. Adv.* **28,** 325–347 (2010).

32. Reneker, D. H., Yarin, A. L., Fong, H. & Koombhongse, S. Bending instability of electrically charged liquid jets of polymer solutions in electrospinning. *J. Appl. Phys.* **87,** 4531–4547 (2000).

33. Shin, Y. M., Hohman, M. M., Brenner, M. P. & Rutledge, G. C. Electrospinning: A whipping fluid jet generates submicron polymer fibers. *Appl. Phys. Lett.* **78,** 1149 (2001).

34. Shin, Y. M., Hohman, M. M., Brenner, M. P. & Rutledge, G. C. Experimental characterization of electrospinning: the electrically forced jet and instabilities. *Polymer (Guildf).* **42,** 09955–09967 (2001).

35. Palmqvist, A. E. C. Synthesis of ordered mesoporous materials using surfactant liquid crystals or micellar solutions. *Curr. Opin. Colloid Interface Sci.* **8,** 145–155 (2003).

36. Abidian, M. R. & Martin, D. C. Multifunctional nanobiomaterials for neural interfaces. *Adv. Funct. Mater.* **19,** 573–585 (2009).

37. Abidian, M. R., Ludwig, K. a., Marzullo, T. C., Martin, D. C. & Kipke, D. R. Interfacing conducting polymer nanotubes with the central nervous system: chronic neural recording using poly(3,4-ethylenedioxythiophene) nanotubes. *Adv. Mater.* **21,** 3764–3770 (2009).

38. Smela, B. E. Conjugated Polymer Actuators for Biomedical Applications. 481–494 (2003).

39. Baughman, R. H., Shacklette, L. W., Elsenbaumer, R. L., Plichta, E. & Becht, C. Conducting Polymer Electromechanical Actuators. *Conjug. Polym. Mater. Oppor. Electron. Optoelectron. Mol. Electron.* 559–582 (1990).

40. Fattahi, P., Borhan, A. & Abidian, M. R. Microencapsulation of chemotherapeutics into monodisperse and tunable biodegradable polymers via electrified liquid jets: Control of size, shape, and drug release. *Adv. Mater.* **25,** 4555–4560 (2013).

41. Zong, X. *et al.* Structure and process relationship of electrospun bioabsorbable nanofiber membranes. *Polymer (Guildf).* **43,** 4403–4412 (2002).

42. Sabouraud, G., Sadki, S. & Brodie, N. The mechanisms of pyrrole electropolymerization. *Chem. Soc. Rev.* **29,** 283–293 (2000).

43. Bredas, J. & Street, G. Polarons, bipolarons, and solitons in conducting polymers. *Acc. Chem. Res.* **1305,** 309–315 (1985).

44. Mabbott, G. a. An introduction to cyclic voltammetry. *J. Chem. Educ.* **60,** 697 (1983).

45. Beasley, C. Basics of Electrochemical Impedance Spectroscopy. *Webinar on EIS of Batteries* (2015). at <http://www.gamry.com/application-notes/EIS/basics-of-electrochemical-impedance-spectroscopy/>

46. Barsoukov, E. & Macdonald, J. R. *Impedance Spectroscopy*. *Impedance Spectroscopy: Theory, Experiment, and Applications* (2005). doi:10.1002/0471716243